Structural Eng./Earthquake Eng. Vol. 10, No. 2, 95s—101s, July 1993
Japan Society of Civil Engineers (J. Struct. Mech. Earthquake Eng. No. 471/I—24)

DYNAMIC RESPONSE ANALYSIS OF STRUCTURE-WATER-GROUND SYSTEMS IN THE TIME DOMAIN USING SEMI-INFINITE ELEMENTS

Fusanori MIURA* and Jun WANG**

The purpose of this study is to propose a simple and accurate numerical method to analyze the dynamic response of structure-water-ground interaction systems in the time domain.

For this purpose, a frequency independent semi-infinite element is newly proposed to model the part of the water system away from the structure. This method is not only suitable for describing the behavior of unbounded water systems, but also for significantly decreasing the number of finite elements. Examples given in this study indicate that the method has excellent computational accuracy and feasibility for analyzing the effects of hydrodynamic pressure on the response of structure-ground interaction systems.

Key Words : *structure-water-ground interaction, semi-infinite element, time domain*

1. INTRODUCTION

In the linear or nonlinear analysis of structure-water-ground systems, such as dams and off-shore structures, which are subjected to seismic excitations, the effect of hydrodynamic pressure has to be taken into account. One of the most powerful tools for analyzing this effect is the finite element method. As the finite element method can only treat finite regions when using it, artificial boundaries must be introduced into the water and ground systems because they extend semi-infinitely. To perform the analyses accurately, we need to take into account the energy absorption at the boundaries due to wave propagation through the boundaries. In time domain analyses hybrid methods with the finite difference method[1),2)] or the boundary element method[3),4)] have previously been applied. These methods are rigorous, however, they need very complicated and elaborate schemes.

In this study, therefore, a simple semi-infinite element method is newly proposed. In this method, a uniform body of water with constant depth extending to infinity is modeled by semi-infinite elements and the viscous boundaries proposed by one of the authors are employed to model the semi-infinitely extending ground[5)]. The traditional semi-infinite element method is used to model the water system in the frequency domain because the distribution of the hydrodynamic pressure depends on the frequency[6)]. The semi-infinite element method proposed in this study, however, is used in the time domain. This means that the proposed method is applicable to nonlinear analyses. A non-linear structure-water-ground interaction analysis method was proposed by one of the authors before, but the semi-infinite extension of the water system was not included[7)].

In chapter 2, we first derive the equation of motion for the analysis of structure-water-ground interaction systems based on a hydrodynamic pressure-acceleration relationship in the time domain. Then, in chapter 3, the semi-infinite element is explained and finally, in chapter 4, the accuracy of the method is examined by using dam-water-foundation models.

2. THE EQUATION OF MOTION

The equation of motion for the analysis of a structure-water-ground system with viscous boundaries is given as follows.

(1) For the structure-ground system :

From previous work by one of the authors (Ref. (5)), the equation of motion for a structure-ground-water-ice interation system is given by :

$$\begin{aligned}&([M]+[M^*])\{\ddot{\delta}\}+([C]+[C_I^L]\\&+[C_I^R]+[C_R^L]+[C_R^R])\{\dot{\delta}\}+[K]\{\delta\}\\&=-([M]+[M^*])\{\ddot{z}_0\}-([C_I^L]+[C_I^R])\{\dot{z}_0\}\\&+([C_R^L]+[C_F^L])\{\dot{x}_F^L\}+([C_R^R]+[C_F^R])\{\dot{x}_F^R\}\\&+[G_F^L]\{x_F^L\}+[G_F^R]\{x_F^R\}\cdots\cdots(1)\end{aligned}$$

where, $[M]$, $[C]$, $[K]$ are mass, damping, and stiffness matrices, respectively. $[M^*]$ is the virtual mass matrix, $\{\delta\}$ is the nodal displacement vector and $\{z_0\}$ is the input ground displacement at the basal layer. The matrices $[C_I^L]$, $[C_I^R]$, $[C_R^L]$, $[C_R^R]$, $[C_F^L]$, $[C_F^R]$ are viscous boundary matrices and $[G_F^L]$ and $[G_F^R]$ are boundary stiffness matrices.

* Member of JSCE, Dr.Eng., Professor, Faculty of Engineering, Yamaguchi University (Tokiwadai, Ube)
** Graduate Student, Faculty of Engineering, Yamaguchi University (Tokiwadai, Ube)

The superscripts L and R denote the "Left" and "Right" boundaries of the model, respectively. The subscripts I, R and F denote "Ice", "gRound", and "Free field", respectively. They are derived by virtue of the principle of virtual work and given in Ref. (5). For the reader's convenience, they are given in the Appendix at the end of this paper. The vectors $\{x_F^L\}$ and $\{x_F^R\}$ are displacement vectors of the free field.

In this study, water-structure and water-ground interaction in terms of hydrodynamic pressure, $\{p\}$ are considered instead of assuming the virtual mass, $[M^*]$. Further, we have not included the contribution of ice, therefor, Eq. (1) is written as :

$$[M]\{\ddot{\delta}\}+([C]+[C_R^I]+[C_R^R])\{\dot{\delta}\}+[K]\{\delta\}$$
$$=-[M]\{a_g\}+[L]\{p\}+([C_R^I]+[C_F^I])\{\dot{x}_F^I\}$$
$$+([C_R^R]+[C_F^R])\{\dot{x}_F^R\}+[G_F^I]\{x_F^I\}+[G_F^R]\{x_F^R\} \quad \cdots\cdots(2)$$

where the input ground acceleration, $\{\ddot{z}_0\}$ is replaced by $\{a_g\}$ and the term $[L]\{p\}$ represents the effect of water, i.e., hydrodynamic pressure. $[L]$ is the transfer matrix from the nodal hydrodynamic pressure of the water system to the nodal forces on the interface between the water system and structure-ground system.

(2) For the water system :

The equation of motion for hydrodynamic pressure is given by[8]

$$[Q]\{\ddot{p}\}+[S]\{\dot{p}\}+[H]\{p\}$$
$$=-\rho_\omega[L]^T(\{a_g\}+\{\ddot{\delta}\}) \quad \cdots\cdots(3)$$

where, $[Q]$, $[S]$ and $[H]$ are the coefficient matrices of second, first and zero order derivatives with time. The matrices $[Q]$ and $[S]$ are related to the compressibility and viscosity. We assumed that the compressibility and viscosity can be neglected, i.e., $[Q]=0$ and $[S]=0$. Based on this assumption, Eq.(3) becomes :

$$[H]\{p\}=-\rho_\omega[L]^T(\{a_g\}+\{\ddot{\delta}\}) \quad \cdots\cdots(4)$$

Equations (2) and (4) are solved by means of Newmark's β-method ($\beta=1/4$). Vectors $\{\delta\}_{n+1}$ and $\{p\}_{n+1}$ at the $(n+1)$ th time step are computed by the following recursion formulas :

$$([M]^*+\frac{1}{2}\Delta t[C]^*+\frac{1}{4}\Delta t^2[K]\{\ddot{\delta}\}_{n+1}$$
$$=\{F\}-[C]^*\{A\}_n-[K]\{B\}_n \quad \cdots\cdots(5)$$

$$[H]\{p\}_{n+1}=-\rho_\omega[L]^T(\{a_g\}_{n+1}+\{\ddot{\delta}\}_{n+1}) \quad \cdots\cdots(6)$$

in which

$$\left.\begin{aligned}[M]^*&=[M]+[L][H]^{-1}\rho_\omega[L]^T\\ [C]^*&=[C]+[C_R^I]+[C_R^R]\end{aligned}\right\}$$

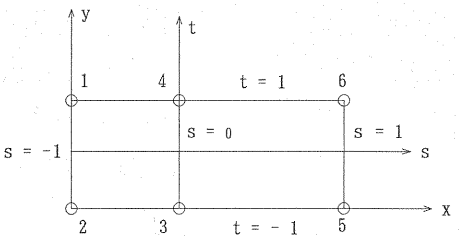

Fig.1 The semi-infinite element

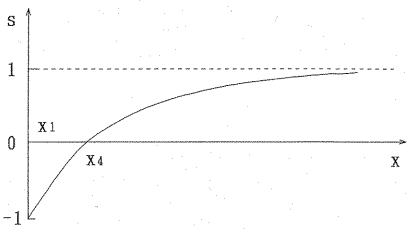

Fig.2 The x-s relation curve

$$\left.\begin{aligned}\{A\}_n&=\{\dot{\delta}\}_n+\frac{1}{2}\Delta t\{\ddot{\delta}\}_n\\ \{B\}_n&=\{\delta\}_n+\Delta t\{\dot{\delta}\}_n+\frac{1}{4}\Delta t^2\{\ddot{\delta}\}_n\end{aligned}\right\} \quad \cdots\cdots(7)$$

It should be noted that the semi-infinite elements which are explained in the following chapter are employed in the water system. Accordingly, the purpose of the next chapter is to derive the matrices $[h]^e$ from which $[H]$ is assembled.

3. THE SEMI-INFINITE ELEMENT

In order to deal with the hydrodynamic pressure in an infinite domain, semi-infinite elements in the time domain are introduced to simulate the effect of the part of the water system away from the structure. Considering the semi-infinite element shown in **Fig.1**, transformations between the global coordinate system (x, y) and the local coordinate system (s, t) of the element are :

$$x=l_1x_1+l_2x_4,\quad y=m_1y_1+m_2y_2 \quad \cdots\cdots(8)$$

where,

$$l_1=-\frac{2s}{1-s},\ l_2=\frac{1+s}{1-s},\ m_1=\frac{1}{2}(1+t),$$
$$m_2=\frac{1}{2}(1-t) \quad \cdots\cdots(9)$$

in which nodes 5 and 6 correspond to $x=\infty$ and $s=1$. The $x-s$ relation curve is shown in **Fig.2**. This curve approaches 1 asymptotically as $x\to\infty$.

The shape functions of the hydrodynamic pressure are employed as follows :

$$p=\sum_{i=1}^{4}w_ip_i \quad \cdots\cdots(10)$$

where,

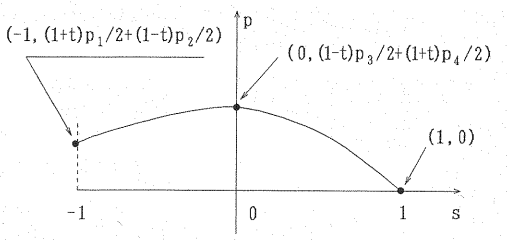

Fig.3 The s-p relation curve

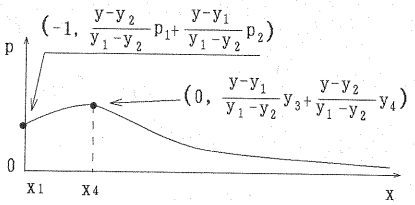

Fig.4 The x-p relation curve

$$\left.\begin{aligned} w_1&=-\frac{1}{4}(1+t)s(1-s),\\ w_2&=-\frac{1}{4}(1-t)s(1-s)\\ w_3&=\frac{1}{2}(1-t)(1+s)(1-s),\\ w_4&=\frac{1}{2}(1+t)(1+s)(1-s) \end{aligned}\right\}\cdots\cdots\cdots\cdots(11)$$

The corresponding s−p curve is shown in **Fig.3**. For the constant t, this curve varies quadratically and is determined by the three points, $(-1, (1+t)p_1/2+(1-t)p_2/2)$, $(0, (1-t)p_3/2+(1+t)p_4/2)$ and $(1, 0)$. When $s=1$ $(x\to\infty)$, $p=0$.

The x−p relation curve is shown in **Fig.4**.In this curve, p asymptotically approaches 0 as $x\to\infty$.

Using the same steps as in the common isoparametric finite element, the semi-infinite element matrix $[h]^e$ can be obtained as follows;

$$[h]^e=\begin{bmatrix} h_{11} & h_{12} & h_{13} & h_{14}\\ h_{21} & h_{22} & h_{23} & h_{24}\\ h_{31} & h_{32} & h_{33} & h_{34}\\ h_{41} & h_{42} & h_{43} & h_{44} \end{bmatrix}\cdots\cdots\cdots\cdots(12)$$

where,

$$h_{ij}=\int\int\left[\frac{\partial w_i}{\partial x}\frac{\partial w_j}{\partial x}+\frac{\partial w_i}{\partial y}\frac{\partial w_j}{\partial y}\right]dxdy$$

$$=\int_{-1}^{1}\int_{-1}^{1}\left[\frac{(1-s)^2(y_1-y_2)}{4(x_4-x_1)}\frac{\partial w_i}{\partial s}\frac{\partial w_j}{\partial s}+\frac{4(x_4-x_1)}{(1-s)^2(y_1-y_2)}\frac{\partial w_i}{\partial t}\frac{\partial w_j}{\partial t}\right]dsdt\cdots\cdots(13)$$

In the above formula, the 2nd term has the factor of $(1-s)^2$ in the denominator, but the factor $(1-s)$ is included in $\partial w_k/\partial t$ $(k=1\sim4)$, therefore, formula (13) has no singular integration and is carried out numerically using Gaussian quadrature without any difficulty.

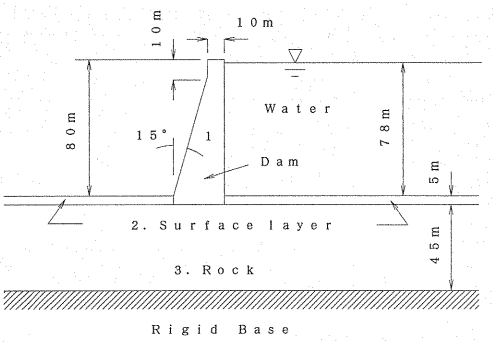

Fig.5 Model of the dam-reservoir-ground system

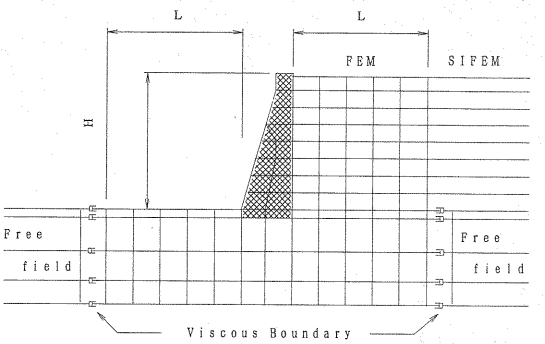

Fig.6 The discretization of the model by finite and semi-infinite elements

4. ANALYSIS RESULTS

(1) Models for the analyses

The model of dam-reservoir-ground shown in **Fig.5** is selected as an example to examine the validity of this analysis method. The discretization of the model by the finite elements (FEM) and the semi-infinite elements (SIFEM) is shown in **Fig.6**.

The dam and the near field parts of the ground and reservoir are discretized by rectangular finite elements. The far field region of the reservoir is modeled by the semi-infinite elements. The effect of semi-infinite regions on both sides of the ground is simulated by the viscous boundaries while the basal layer beneath the ground is regarded as rigid. The relevant physical parameters are given in **Table 1**. For the examination of the applicability of the semi-infinite element, the four cases, A, B, C and D, in **Table 2** are studied. In cases A, B and C, the semi-infinite elements in **Fig.6** are not used and the corresponding boundaries are free. The natural frequencies of the four cases were obtained from the resonant curves and were all 1.80 Hz approximately, as shown in the following section.

Table 1 The physical parameters of the model

	Unit weight (ton.f/m³)	Shear wave velocity (m/sec)	Poisson's ratio	Damping ratio	c (c') (ton.f/m²)	ϕ(ϕ') (°)
1. Dam	2.4	2046	0.17	0.1		
2. Surface layer	1.9	158	0.4	0.05	8	10
3. Rock	2.8	3300	0.3	0.1		
4. Water	1.0	incompressibility				

Table 2 The analyzing cases

Case	L	Semi-infinite element
A	H	without
B	2H	without
C	3H	without
D	H	with

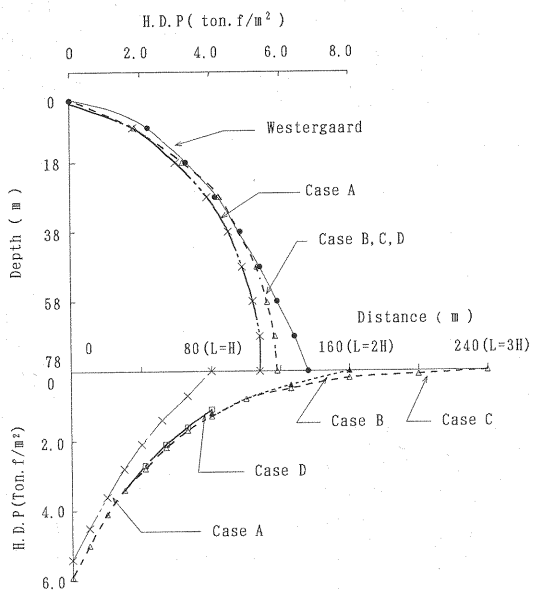

a. f=0.5 Hz

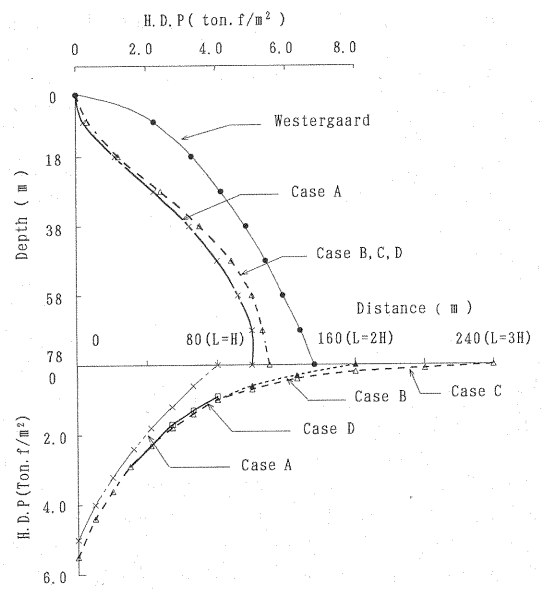

c. f=5.0 Hz

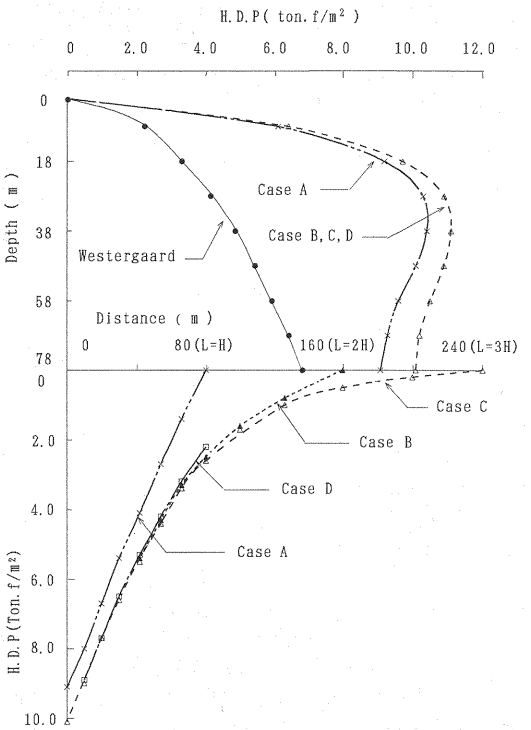

b. f=1.80 Hz

Fig.7 The distribution of the maximum hydrodynamic pressure along the upstream face of the dam and the bottom of the reservoir for harmonic excitation

The natural frequency of the dam-foundation system without water is about 2.34 Hz.

(2) Response to harmonic excitations

Sinusoidal acceleration with the amplitude of 100 gal and with frequencies from 0.5 Hz to 8.0 Hz were chosen as the input at the base of the ground.

Figs.7a, 7b and **7c** compare the distributions of the maximum hydrodynamic pressure along the upstream face of the dam and the bottom of the reservoir in all four cases at 0.5 Hz, 1.80 Hz and 5.0 Hz, respectively. In these figures, results from the corresponding Westergaard's equation (100 gal)

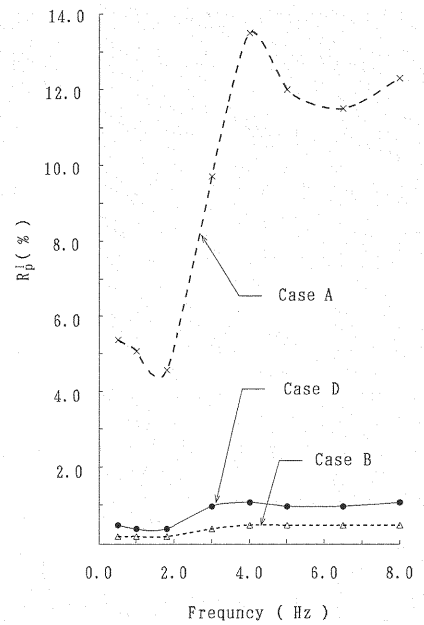

Fig.8 The relative errors of the maximum hydrodynamic pressure

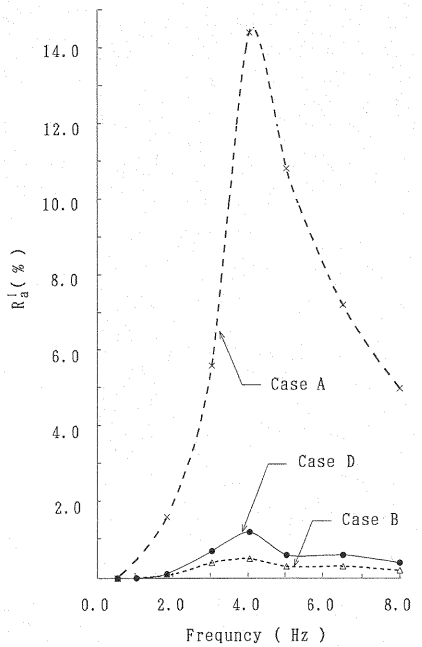

Fig.9 The relative errors of the maximum acceleration

are also shown. The figures clearly show that at the same frequency, the magnitude of the hydrodynamic pressure in Cases B, C and D, is very much alike, especially along the upstream face of the dam, and the magnitude of Case A is obviously smaller than those of the other three cases.

In more detail, **Fig.8** shows the relative errors of the hydrodynamic pressure from Cases A, B and D, to that from Case C. The relative errors R_p^I are determined by the following equation.

$$R_p^I=\frac{p_{Case\ C}-p_{Case\ I}}{p_{Case\ C}}\times 100\% \quad \cdots\cdots\cdots\cdots\cdots\cdots (14)$$

where I=A, B, or D. $p_{Case\ C}$ means, for example, the maximum hydrodynamic pressure at the 3/4 height point of the upstream face of the dam for Case C.

The relative error for Case A is more than 10% and is very large compared with the other cases, especially for the frequencies higher than 4.0 Hz. The relative error for Case D, which has the same L as Case A, is at most 1%. This indicates the efficiency of the semi-infinite elements.

The same behavior can be obtained for the acceleration responses. **Fig.8** describes the corresponding results, in which, the relative errors R_a^I are given by :

$$R_a^I=\frac{a_{Case\ C}-a_{Case\ I}}{a_{Case\ C}}\times 100\% \quad \cdots\cdots\cdots\cdots\cdots\cdots (15)$$

where, $a_{Case\ C}$ means, for example, the maximum acceleration at the 3/4 height point of the upstream face of the dam for Case C.

As shown in the previous chapter, the shape function of the semi-infinite element does not include the frequency. It means that the accuracy of the responses from the model with the semi-infinite elements may be independent of the excitation frequency.

Fig.8 and **Fig.9** indicate that the keen peak at frequency about 4 Hz, which is predominant in Case A, disappears in Case D. Therefore, we recognize that the frequency-independent semi-infinite element provides a high level of accuracy irrespective of the excitation frequency.

(3) Responses to the seismic accelerogram excitations

The NS component of El Centro accelerogram (max. is 342 gal) and the Pasadena record from the 1952 Kern County earthquake (max. is 57 gal) are used as input motions. The distribution of the maximum hydrodynamic pressure for Cases A, B, C, D and from Westergaard's equation, are shown in **Fig.10a** and **Fig.10b**. The distribution of the maximum acceleration for Cases A, B, C and D, are shown in **Fig.11a** and **Fig.11b**. The figures show once again that the responses of Cases B, C and D, are nearly the same, and the responses of Case A are smaller than those of the other three cases as discussed in the above section.

For the El Centro input motion, the relative error of the hydrodynamic pressure for Case C at the foot of the dam is 8.4% for $L=H$ (FEM), 1.7%

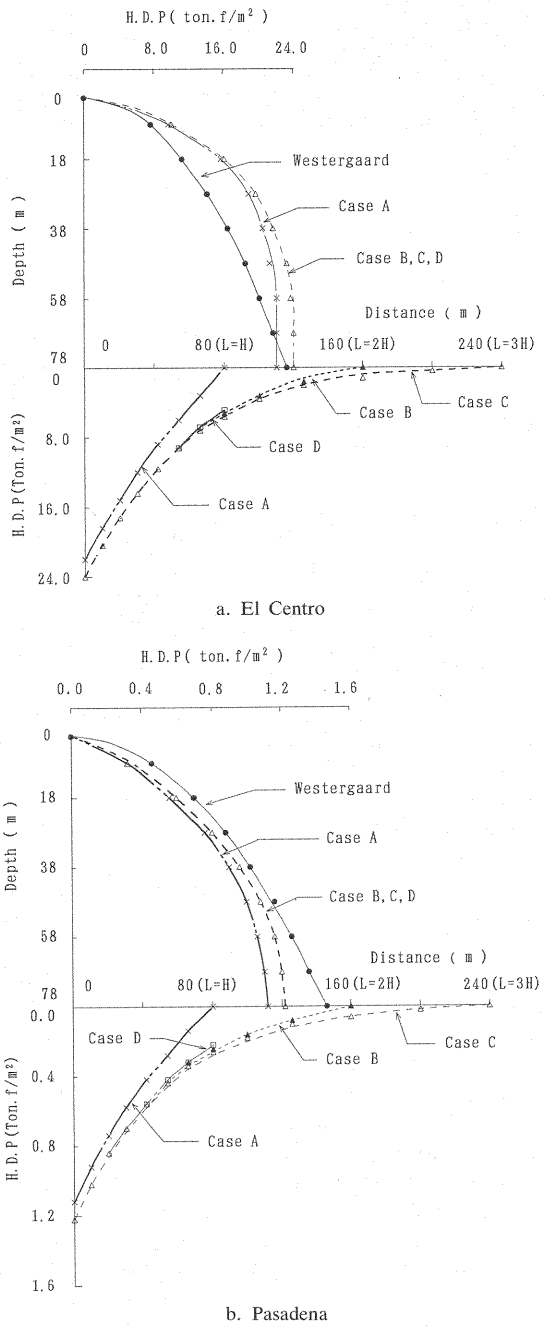

Fig.10 The distribution of the maximum hydrodynamic pressure along the upstream face of the dam for the accelerogram excitation

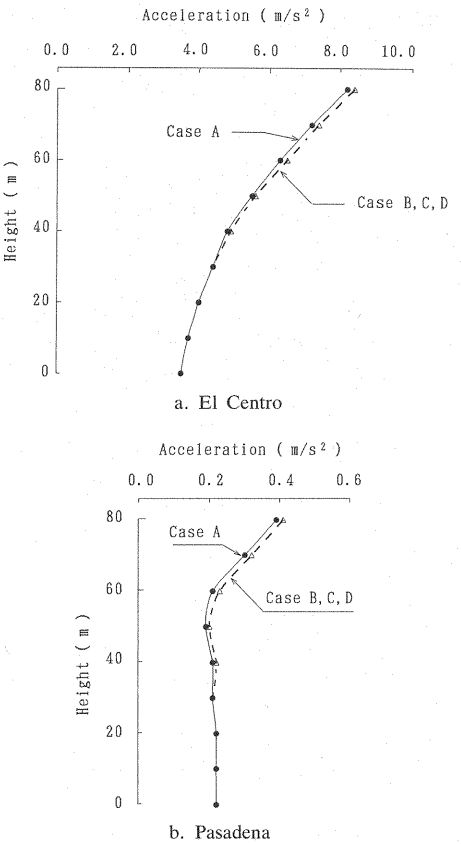

Fig.11 The distribution of the maximum acceleration at the upstream face of the dam subjected to accelerogram excitations

for $L=1.5H$ (FEM), and less than 0.7% for $L=H$ (SIFEM) and $L=2H$ (FEM), while the relative error of the acceleration response for Case C at the top of the dam is 2.6% for $L=H$ (FEM), 1.0% for $L=1.5H$ (FEM), and less than 0.1% for $L=H$ (SIFEM) and $L=2H$ (FEM).

For the Pasadena input motion, the above relative error for the hydrodynamic pressure is 8.1% for $L=H$ (FEM), 1.6% for $L=1.5H$ (FEM), and less than 0.7% for $L=H$ (SIFEM) and $L=2H$ (FEM), while that of the acceleration response, is 2.8% for $L=H$ (FEM), 0.7% for $L=1.5H$ (FEM), and less than 0.1% for $L=H$ (SIFEM) and $L=2H$ (FEM). And, the cpu time by EWS (SUN S-4/2) for the model with $L=H$ (SIFEM) is 55.1 sec. and this is much less than that with $L=2H$ (FEM) of 73.9 sec..

Thus, it may be expected that the same precision can be achieved by means of the model with $L=H$ (SIFEM) and with $L=2H$ (FEM). Therefore, the number of elements can be decreased significantly if the semi-infinite elements are used.

5. CONCLUSIONS

A rather simple and practical method which is effective in time domain analysis, is developed for structure-water-ground interaction analysis.

A generalized semi-infinite element method is suggested to evaluate the hydrodynamic effect of

far field water on a structure. The advantage of the method is that it reduces the computational effort to a great extent, while it ensures the required accuracy.

APPENDIX

(1) Viscous Boundary Matrix $[C_R]$

The viscous boundary matrix for the (i) th element of which nodes are i and $i+1$ as shown in **Fig. A.1** is given by

$$[C_R]_i=\frac{\rho H}{6}\begin{bmatrix} 2V_p & 0 & V_p & 0 \\ 0 & 2V_s & 0 & V_s \\ V_p & 0 & 2V_p & 0 \\ 0 & V_s & 0 & 2V_s \end{bmatrix} \quad \cdots\cdots (A\cdot 1)$$

where, ρ, H, V_p and V_s are the mass denisity, the element height, the P wave velocity and the S wave velocity of the (i) th element, respectively. $[C_R]$ is assembled from the materices $[C_R]_i$ in standard fashion. Here, we have the relation as follows:

$$[C_R^L]=[C_R^R] \quad \cdots\cdots (A\cdot 2)$$

(2) The boundary stiffness matrix $[G_F]$ and the boundary viscous matrix $[C_F]$

$[G_F]_i$ for the (i) th element at the boundary is given by

$$[G_F]_i=\frac{1}{2}\begin{bmatrix} 0 & -\lambda & 0 & \lambda \\ -\mu & 0 & \mu & 0 \\ 0 & -\lambda & 0 & \lambda \\ -\mu & 0 & \mu & 0 \end{bmatrix} \quad \cdots\cdots (A\cdot 3)$$

where, λ, μ are the Lame's constants. $[G_F]$ is also assembled from $[G_F]_i$ as above. And,

$$[G_F^L]=-[G_F^R] \quad \cdots\cdots (A\cdot 4)$$

Rayleigh damping is assumed for the matrices $[C_F]_i$ and therefore,

$$[C_F^L]=\frac{h}{\pi f}[G_F^L],\ [C_F^R]=\frac{h}{\pi f}[G_F^R] \quad \cdots\cdots (A\cdot 5)$$

in which, h is the damping coefficient of frequency, f.

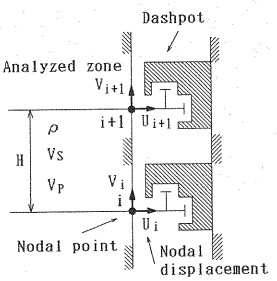

Fig.A.1 The model of viscous boundary and the symbols related to it

REFERENCES

1) Shiojiri, H. and T. Taguchi : The development of a seismic response analysis method of concrete gravity dams, Civil Engineering Laboratory, Rep. No.385012, 1985.
2) Priscu, R., Popovici, A., Ilie, L. and Stematiu, D. : New aspects in the earthquake analysis of arch dams, Criteria and assumption for numerical analysis of dams, ED by Nalor, D.N. et al., Proc. Int. Symp., Swansea, United Kingdom, Sept., pp.709~725, 1975.
3) Touhei, T. and T. Ohmachi : A FE-BE method in time domain for dynamic response analysis of dam-foundation-reservoir systems, Proc. of the J.S.C.E., No,422, pp.381~390, 1990.
4) Wepf, D.H. and Wolf, J.P. : Time domain dam-reservoir-interaction analysis based on boundary element, Proc. of China-U.S. Workshop on Earthquake behavior of arch dams, pp.130~147, June, 1987.
5) Miura, F., I. Nozawa, N. Sakaki and K. Hirano : The Effect of Ice on the Seismic Response and Dynamic Stability against Sliding of Off-shore Structures, Proc. of the J.S.C.E., No.409, pp.65~73, 1989.
6) Zienkiewicz, O.C. and Bettess, P. : Coupled hydrodynamic response of concrete gravity dams using finite element method and infinite element, EESD, Vol.6, pp.363~374, 1978.
7) Toki, K., F. Miura and M. Terada : Seismic response analyses of the water-soil-revetment structure interaction system, Annual Report of the Disaster Prevention Research Institute, Kyoto Univ., No.25, B-2, pp.67~83, 1982.
8) Zienkiewicz, O.C. : The finite element method, 3 rd ed., ch 20, pp.540, 1982.

(Received July 6. 1992)